Variability of rainfall over Lake Kariba catchment area in the Zambezi river basin, Zimbabwe

Shepherd Muchuru · Joel O. Botai · Christina M. Botai · Willem A. Landman · Abiodun M. Adeola

Abstract In this study, average monthly and annual rainfall totals recorded for the period 1970 to 2010 from a network of 13 stations across the Lake Kariba catchment area of the Zambezi river basin were analyzed in order to characterize the spatial-temporal variability of rainfall across the catchment area. In the analysis, the data were subjected to intervention and homogeneity analysis using the Cumulative Summation (CUSUM) technique and step change analysis using rank-sum test. Furthermore, rainfall variability was characterized by trend analysis using the non-parametric Mann-Kendall statistic. Additionally, the rainfall series were decomposed and the spectral characteristics derived using Cross Wavelet Transform (CWT) and Wavelet Coherence (WC) analysis. The advantage of using the wavelet-based parameters is that they vary in time and can therefore be used to quantitatively detect time-scale-dependent correlations and phase shifts between rainfall time series at various localized time-frequency scales. The annual and seasonal rainfall series were homogeneous and demonstrated no apparent significant shifts. According to the inhomogeneity classification, the rainfall series recorded across the Lake Kariba catchment area belonged to category A (useful) and B (doubtful), i.e., there were zero to one and two absolute tests rejecting the null hypothesis (at 5 % significance level), respectively. Lastly, the long-term variability of the rainfall series across the Lake Kariba catchment area exhibited non-significant positive and negative trends with coherent oscillatory modes that are constantly locked in phase in the Morlet wavelet space.

S. Muchuru (correspondence) · J. O. Botai · W. A. Landman · A. M. Adeola Department of Geography, Geoinformatics and Meteorology, University of Pretoria, Pretoria, South Africa
e-mail: shephido@yahoo.com

C. M. Botai
South African Weather Service, Private Bag X097, Pretoria 0001, South Africa

W. A. Landman
Council for Scientific and Industrial Research, Natural Resources and the Environment, Pretoria, South Africa

1 Introduction

Rainfall is one of the climatic variables that affect both the spatial and temporal patterns on water availability (De Luis et al. 2000; Kampata et al. 2008; Ngongondo 2006). In particular, the southern African region experiences significant rainfall variability at various spatial and temporal scales and is prone to serious drought and flood events (e.g., Tysen 1986; Nicholson and Entekhabi 1987; Lindesay 1988; Reason et al. 2000). The region is characterized by the increasing changes in high rainfall events (Mason and Joubert 1997), and it is also most sensitive to precipitation shifts and variability (IPCC 2007). The variability of rainfall over southern Africa can have detrimental consequences to economic development, disaster management, population, and hydrological planning of a particular country. Due to anomalous rainfall variability, major water resources and reservoirs are often at risk (e.g., due to flooding), and the population and properties in the basin are often impacted most.

The region's water resources, agriculture, and rural communities are impacted considerably due to high rainfall variability (Cook et al. 2004). It is imperative to perform spatial temporal variability analysis of rainfall at monthly or seasonal timescales to determine the likelihood of extreme (drought or flood) events occurrences and or return periods. For example, the identification of seasons in which floods are most likely involves studying characteristics of monthly rainfall within the seasons across the region. To this end, better understanding of the relationships between rainfall and other climatic variables contributes towards water resource management

and planning. It is therefore essential to thoroughly study rainfall variability at monthly, seasonal, and annual time scales in order to support the management of water resources (Nsubuga et al. 2011). As reported in Mason and Jury (1997), precipitation in southern African exhibits high variability at all timescales. This variability has been attributed to the proximity of the Agulhas, Benguela, and Antarctic circumpolar currents, which are characterized by complex and highly variable climate patterns around southern Africa (Shannon et al. 1990). Further, the 1984 floods along the Namibian coast for instance were associated with extremely warm SST in the Angola/Benguela front region typical of the Benguela Niño. In addition, the 2000 floods which hit Mozambique, eastern Zimbabwe and northeast South Africa could have been influenced by the Tropical-Temperate Troughs (TTTs) which have been previously linked to high rainfall intensities. Further, the El Niño Southern Oscillation (ENSO) has also been associated to major floods and drought events in the southern African region (e.g., Cook 2000; Mason and Jury 199; Reason and Rouault 2002).

Several studies investigating rainfall variability in the Zambezi river basin have been reported in the literature. For example, Mazvidza et al. (2000) grouped the precipitation records of the Lake Kariba catchment using a number of Zambian weather stations into decadal means between 1960 and 1990 to determine climate change and variability. Records from ten of the 15 examined stations showed the 1980–1990 decade experienced the lowest means of flows over the last 40 years, while 15 stations registered the lowest mean of flow for the past 30 years in the same decade. Mazvimavi and Wolski (2006) analyzed the trends of rainfall, stream flow, and long-term variations of annual flows of the Okavango and Zambezi rivers for the period of 1933–2004 and 1924–2004, respectively. The maximum and minimum annual flows of the Okavango and Zambezi rivers were analyzed and found to have inherent exhibit change points. In addition, Kampata et al. (2008) analyzed long-term rainfall data in the headstream regions of the Zambezi river basin using the Cumulative Summation (CUSUM technique), step change analysis, and Mann-Kendall statistics to study the spatial-temporal variability of rainfall between 1935 and 2006. From the analysis, Kampata et al. (2008) reported that the rainfall data in the entire sub-basin belonged to a similar climate regime, and the trends observed at the different stations were homogeneous.

Notwithstanding the valuable contribution of the above studies towards our understanding of spatial-temporal variability of rainfall in the larger Zambezi river basin, analysis of the variability of rainfall in the Kariba catchment area remains inconclusive. This study focuses on the Lake Kariba catchment region in the Zambezi river basin since rainfall over this area influences all important processes responsible for, e.g., hydroelectricity, agriculture, and livestock. Lake Kariba catchment climatology is controlled mainly by the movement of air masses associated with the Inter-Tropical Convergence Zone (ITCZ) (Beilfuss 2012). Normally, the rainy season extends from November to March. The entire catchment is highly susceptible to extreme droughts and floods that occur nearly every decade (Beilfuss 2012), but these has become more frequent and more pronounced with associated economic losses (Solomon et al. 2007). For example, during the severe 1991/1992 drought, reduced hydropower generation resulted in an estimated US$102 million reduction in GDP, $36 million reduction in export earnings, and the loss of 3000 jobs. Extreme floods have also resulted in considerable loss of life, social disruptions, and extensive economic damage. The purpose of this study is to characterize rainfall variability across the Kariba catchment through intervention analysis, homogeneity tests, trend analysis as well as spatial and spectral correlation analysis using wavelet-based parameters. Characterizing rainfall variability and trends can be used for decision making and further hydrological modeling.

2 Study area

Lake Kariba is one of the largest artificial reservoirs (by volume) in the world with a surface area of 5577 km^2 and a live storage volume 564,800 Mm^3 (Beilfuss 2012). Lake Kariba regulates runoff from an upstream catchment area of 687, 535 km^2, which is about 50 % of the total Zambezi catchment area. Average annual rainfall for the Lake Kariba catchment area (see Fig. 1) is about 1000 mm, producing a mean annual discharge of 37,249 Mm^3 (and an average flow rate of 1181 $mm^3\ s^{-1}$). Approximately 50 % of annual rainfall over the catchment, on average, contributes to Zambezi base flow (Sharma and Nyumbu 1985; Beilfuss 2012). During drought years, the magnitude and duration of average peak flows may be reduced by 70 % or more. Runoff varies considerably from year to year, e.g., from a remarkable 72,800 Mm^3 in 1957/1958 to as low as 12,300 Mm^3 in 1995/1996. The time series of annual flows reveals long-term cycles of high, medium, and low runoff. These cycles also influence runoff. For instance, a sequence of particularly low rainfall years in the catchment, such as the one that occurred during the early 1900s and again during the period 1980 to1998, can significantly reduce the proportion of annual rainfall that occurs as runoff (Beilfuss 2012).

3 Data and methodology

3.1 Data

Monthly total rainfall data considered in the present study consists of observations from a network of 13

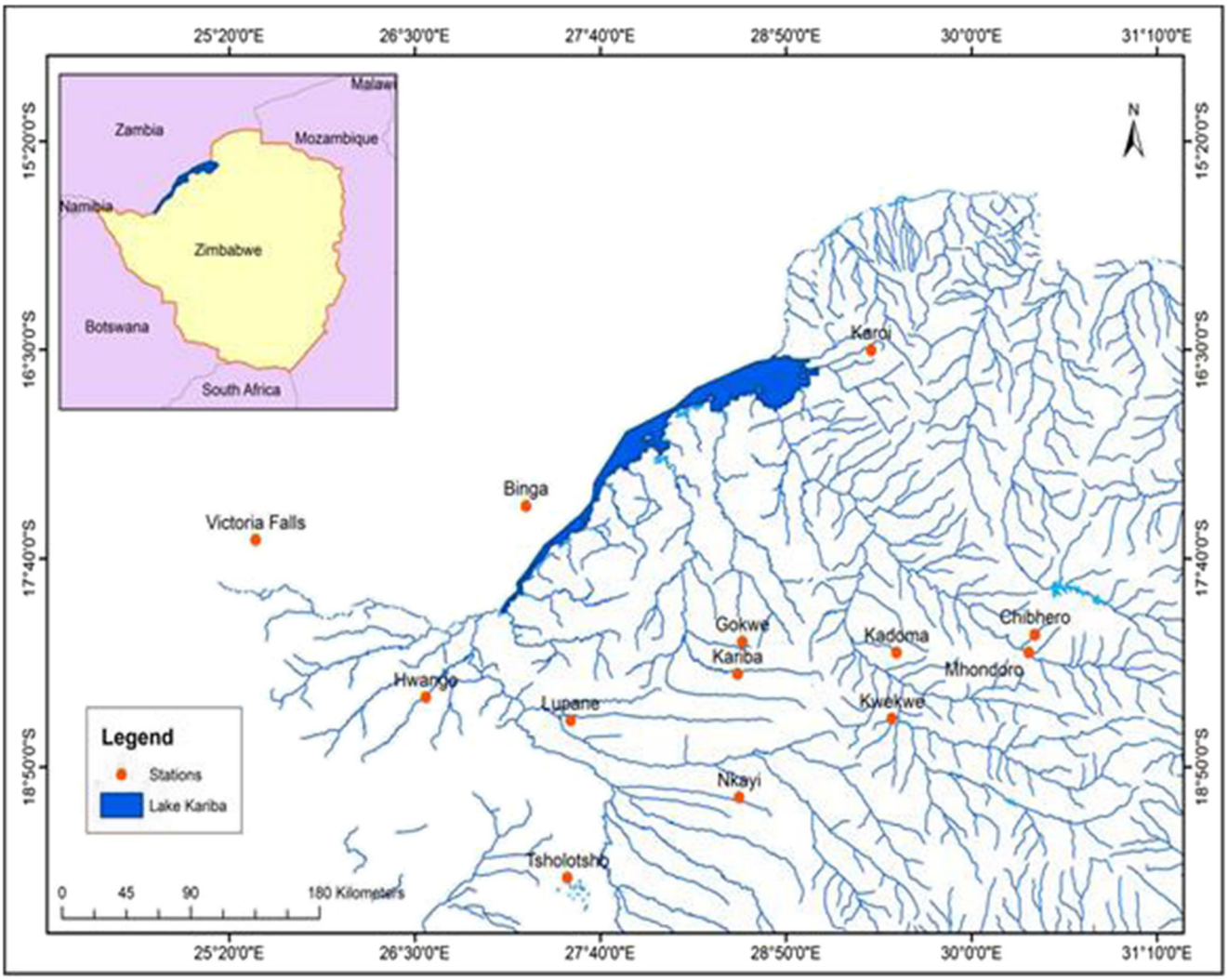

Fig. 1 Location of the Kariba River Basin and some of the meteorological stations

stations which are distributed across the Lake Kariba catchment area. These data sets were obtained from Zimbabwe Meteorological Services (ZMS). Furthermore, these monthly total rainfall data records spanned a period of 1970 to 2010 without any missing data sets. Table 1 summarizes the characteristics of the selected stations.

3.2 Methodology

3.2.1 Intervention and homogeneity

Rainfall data collected at stations spanning a period of several years may not be homogeneous, i.e., the rainfall measurements may have inherent sudden changes or shifts in its mean and variance in relation to the original values. These inhomogeneities and inconsistencies may occur due to several causes, some of which are related to changes in (a) sensor instrumentation (malfunctioning, variation in the power supply, and even replacements), (b) observation practices (including changes in observation times, location of the instrument), (c) modifications of the environmental conditions (overall changes in land cover and land use) of the site, and (d) overall climate change and variability. As a result, observations made prior to the changes often exhibit different statistical properties than data sets collected after the change. As a first step towards understanding the variability of rainfall in a given area, it is necessary to apply appropriate techniques to evaluate whether a given data set can be considered to be homogeneous and, if not, introduce the appropriate corrections. In the present study, intervention and homogeneity analysis approaches are considered. A Cumulative Summation (hereafter CUSUM) technique reported in, e.g., Parida et al. (2003) and Kampata et al. (2008)

Table 1 Characteristics of the study network of stations

Geographical location	National number	Station name	Latitude (°)	Longitude (°)
Mashonaland West	67,891	Mhondoro Met	−18.19	30.36
Mashonaland West	67,893	Chibhero Met	−18.09	30.40
Mashonaland West	67,761	Kariba Airport Met	−16.31	28.53
Matebeleland North	67,843	Victoria Falls Met	−17.56	25.50
Midlands	67,865	Kwekwe Met	−18.56	29.50
Mashonaland North	67,869	Kadoma Met	−18.19	29.53
Mashonaland West	67,765	Karoi Met	−16.50	29.37
Matebeleland North	67,853	Hwange Met	−18.44	26.57
Midlands	67,861	Gokwe Met	−18.13	26.56
Matebeleland North	67,755	Binga Met	−17.37	27.20
Matebeleland North	67,857	Tsholotsho Met	−19.45	27.46
Matebeleland North	67,855	Lupane Met	−18.57	27.48
Matebeleland North	67,863	Nkayi Met	−19.00	28.54

expressed in Eq. (1) was used to decipher the inconsistencies and test for homogeneity across the network of 13 stations of the Kariba catchment region depicted in Fig. 1.

$$S_m = S_{m-1} + (x_m - x_{\text{mean}}), m = 1, 2, ..., n \quad (1)$$

In Equation, S_m is the CUSUM value, x_{m} is the mean of n data points. Dates when the S_m values change between positive and negative values are used to split the data set into two periods, i.e., the pre- and post-intervention periods. The resulting data groups are then subjected to a step change analysis using the rank-sum test (which is a non-parametric test, the median differences between two data subsets) reported in, e.g., Helsel and Hirsch (2002). The relevant equations for the rank-sum test statistic Z_{rs} have been summarized in Kampata et al. (2008) and re-written in Eq. 2 for the purpose of completeness.

$$Z_{rs} = \begin{cases} \frac{S_m - 0.5 - \mu_t}{\sigma} & \text{if } S_m > \mu_t \\ 0 & \text{if } S_m = \mu_t \\ \frac{S_m - 0.5 - \mu_t}{\sigma} & \text{if } S_m < \mu_t \end{cases} \quad (2)$$

$$\mu_t = 0.5k(N+1)$$

$$\sigma = \sqrt{\frac{km(N+1)}{12}}$$

In Eq. 2, S_m, μ_t, and σ are the statistic (computed as the sum of ranks of the observations in the smaller group), the theoretical mean, and standard deviation, respectively, of ranked data. Furthermore, N is the largest rank while k and m are the number of observations in the smallest and largest group, respectively. When $Z_{rs} < Z$ (Z is the critical value of the Z-statistics obtained from the normal distribution table at a 5 % significance level; see Kampata et al. 2008), then the null hypothesis, H_0, is accepted suggesting that the two samples come from the same distribution.

As reported in Peterson et al. (1998), there are numerous methods used to assess the heterogeneity in a time series. It is, however, recommended that a combination of statistical and metadata information be considered during analysis of homogeneity in order to effectively track down any inherent heterogeneity in, e.g., rainfall time series. Furthermore, homogeneity can be assessed by use of relative or absolute methods (Sahin and Cigizoglu 2010). As reported in Sahin and Cigizoglu (2010), relative methods of detecting homogeneity in a time series assume that the reference station is homogeneous and often require the series at each candidate stations to be correlated. In cases where the correlation is low, absolute methods (which often utilize individual station time series) are considered more tractable (Wijngaard et al. 2003).

Absolute statistical methods such as those reported in, for example, Peterson et al. (1998), Alexandersson (1986), and Costa and Soares (2009) have been widely used for homogeneity tests. These methods often vary in complexity and assumptions of the statistical properties of the data series. For a detailed algorithm of these tests, the reader is referred to Wijngaard et al. (2003) and references therein. In the present work, the four main absolute methods widely used for homogeneity test are considered and are summarized in Table 2. In the SNHT, BRT, and PT, an inherent step-wise shift in the mean often designates an inhomogeneous series and the test is capable of locating the corresponding breakdown time (i.e., these tests are location specific). Furthermore, a classification of the test results reported in Wijngaard et al.

Table 2 Absolute statistical methods of homogeneity test

Type of test	Null hypothesis	Remarks
Standard normal homogeneity test (SNHT)	H_0: The whole series is homogeneous, i.e., $z_i \in N(0,1)$; $i \in (1....n)$ H_1: Series is inhomogeneous i.e., $z_i \in \begin{cases} N(\mu_1, 1); & i \in (1....a) \\ N(\mu_2, 1); & i \in (a+1....n) \end{cases}$	– Alexandersson (1986) and Alexandersson and Moberg (1997) – Can be used to account for more than one discontinuity, testing for inhomogeneous trends rather than just breaks, and inclusion of change invariance
Buishand range test (BRT)	H_0: Precipitation follows one or more distributions that have the same mean H_1: there exists a time t the precipitation changes the mean	– Buishand (1982) – Use adjusted partial sums: $S_0^* = 0$, $S_y^* = \sum_{i=1}^{y} \left(Y_i - \overline{Y}\right), \quad y = 1, 2...., n$ – When the value of S_y^* oscillates around zero, then the data is homogeneous – A rescaled range is computed as $R = \frac{\max S_y^*}{0 \le y \le n} - \frac{\min S_y^*}{0 \le y \le n}$
Pettit test	H_0: Data are homogeneous H_1: A date at which there is change in the data exists	– Pettit (1979) – This test is based on the rank, r_i of Y_i, and ignores the normality of the series $X_y = 2\sum_{i=1}^{y} r_i - y(n+1), \quad y = 1, 2, \ldots n$ – The break occurs in year k when $X_k = \max_{1 \le y \le n} \left\lvert X_y \right\rvert$
von Neumann ratio test (VNRT)	H_0: precipitation data sets are independent, identically distributed randomly and that for homogeneous precipitation, the mean of the ratio is two H_1: there is a date at which there is a change in precipitation	– von Neumann (1941) – It is a test that used the ratio of mean square successive (year to year) difference to the variance – Test statistic: $N = \frac{\sum_{i=1}^{n-1} (Y_i - Y_{i+1})^2}{\sum_{i=1}^{n} (Y_i - Y_{\text{mean}})^2} \frac{N}{N-1}$

(2003) has also been considered to characterize the nature of homogeneity across the stations used in this study.

3.2.2 Trend analysis

In this study, trend analysis was done using the non-parametric Man-Kendall (MK) test (Mann 1945; Kendall 1975). In particular, the trend magnitudes were computed by the Theil-Sen's estimator (Theil 1950; Sen 1968). The MK test has been widely used in hydro-meteorological time series to detect significant trends (Yue and Hashimo 2003; Cannarozzo et al. 2006; Partal and Kahya 2006; Mazvimavi and Wolski 2006; Modarres and da Silva 2007; Kampata et al. 2008; Liu et al. 2008) and highly recommended by the World Meteorological Organization (WMO). The authors feel that it suffices just to mention the MK null hypothesis herein and the readers are encouraged to refer to the existing numerous literature for relevant equations of the MK test statistic.

3.2.3 Wavelet-based coherence analysis

One practical application of wavelet analysis in interpreting multiscale, irregular, non-stationary, and noisy time series as well as analyzing the transient coupling between any two signals has been demonstrated and reported in numerous literature (see for example, Torrence and Compo 1998; Grinsted et al. 2004; Maraun and Kurths 2004; Maraun et al. 2007). In order to characterize the causal relationships (such as localized variability, dominant modes of variability, and their time evolution) of precipitation across the study network in the Kariba catchment area (which are thought to be linked together by similar climatology), rainfall records at each station were decomposed into time-frequency space based on the procedure described in Torrence and Compo (1998). In the present work, the continuous wavelet transform was used to expand the annual precipitation time series into the wavelet space in order to detect and characterize any inherent intermittent variability (Torrence and Compo 1998; Grinsted et al. 2004;

Maraun and Kurths 2004; Maraun et al. 2007). In addition, the Cross Wavelet Transform coefficients (CWTs) were constructed from pairs of continuous wavelet transform coefficients (station-wise pairs). The CWTs are suitable for divulging common power and relative phases present in the time series in the wavelet space. In order to reveal significant coherence (even in cases of low common power) of the paired station-wise precipitation records, the Wavelet Coherence (WC) between any two CWT was computed and analyzed using a methodology reported in, e.g., Grinsted et al. (2004) and Maraun and Kurths (2004). Overall, the advantage of using wavelet-based parameters (i.e., CWT and WC) is that they vary in time and therefore can detect the association between different modes of climate fluctuation as well as provide the localized linear correlation of pairs of climate fluctuation at a specific frequency and time in the wavelet space. The statistical significance of the computed CWT and WC were estimated using the Monte Carlo method reported in Grinsted et al. (2004).

4 Results and discussion

4.1 Rainfall variability in the Kariba catchment area

Understanding and explaining the nature and causes of quasi-regular spatial-temporal variability in precipitation has been central in hydro-meteorology, climate, and weather research. In the first phase of analyzing rainfall variability in the Kariba catchment region, graphical visual examination of the data sets was carried out in order to flag any biases (this is determined statistically by use of standard deviation as the thresholds) and record the number of missing data sets. In general, the data sets used in the present study were good and the proportion of missing data was less than 0.5 % in most of the stations. As shown in Fig. 2, the pattern or structure of, e.g., the monthly rainfall variability across the study network is strikingly similar albeit systematic differences in the amplitudes of the modes of variability across the stations and at different timescales.

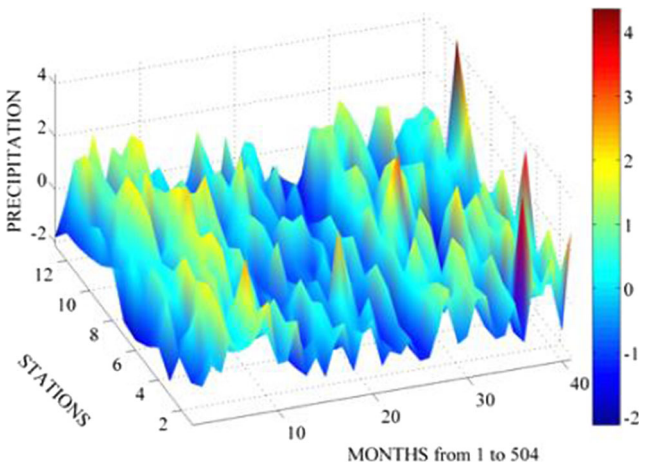

Fig. 2 Visual inspection of rainfall variability

Time box plots depicted in Fig. 3 were used to analyze the characteristic variability of rainfall across all the stations. As illustrated in Fig. 3, all the stations exhibit very similar decadal variability pattern as there are no noticeable differences in the decadal medians. The long upper whisker could be associated to the presence of extreme values and or outliers (biases) in the data sets. The seasonally averaged rainfall totals clearly depict that summer rainfall (DJF) is also 50 % higher than winter (JJA), which, as expected, has the lowest rainfall. The variability during winter is at the minimum (short whiskers). The seasonal pattern of rainfall in the Kariba catchment region is demonstrated by the bottom panel of Fig. 3. As shown in Fig. 3, the Kariba catchment area receives rainfall between November and March with extreme rainfall events or suspected station-dependent interventions recorded in across most months except for January and November.

Investigating whether the rainfall series exhibits a normal distribution is vital in order to determine whether parametric or non-parametric tests would be used for assessing the presence of interventions, homogeneities, trends, and variability. In order to understand the underlying distribution characteristics of the monthly rainfall, DJF, and annual averaged rainfall totals, four normality tests—Shapiro-Wilk (SW), Anderson-Darling (AD), Lilliefors (LF), and Jarque-Bera (JB) tests (see for example Quesenberry 1986); Razali and Wah 2011)—were applied to the rainfall data sets. The results of these tests are given in Table 3. As illustrated in Table 3, the normality of rainfall data was confirmed by two and four tests only in Victoria Falls and Tsholotsho stations, respectively. Data from six stations were confirmed normally distributed from all the tests. The percentage number of stations confirmed to be normally distributed varied from test to test as follows: JB (85 %), LF (81 %), AD (81 %), and SW (65 %). Two important conclusions can be drawn from results given in Table 3. Firstly, the test for normality across by use of four normality tests yields different tests for the different time series of interest, i.e., annual or seasonal. These inherent differences arise due to the differences in the data records as well as the differences in the underlying geophysical processes that drive rainfall variability. Notwithstanding these differences, confirmation of normality in the rainfall totals is important as it avers to the use of non-parametric methods for intervention, homogeneity, and trend analysis as appropriate in the present study.

4.2 Intervention and homogeneity analysis

4.2.1 Intervention analysis

The rainfall CUSUM values for 12 of the 13 stations depicted in Fig. 4 demonstrate that the monthly rainfall has been above

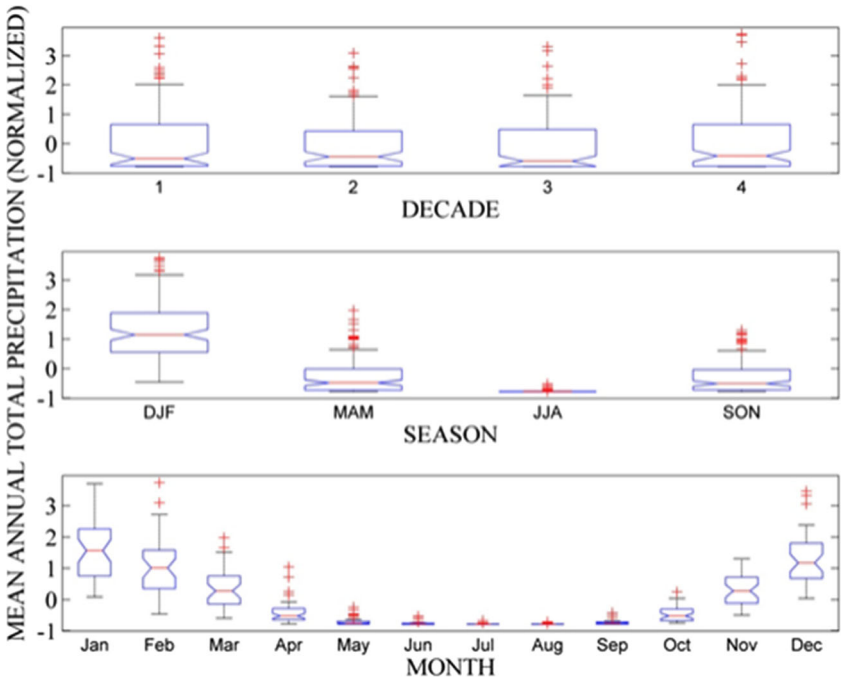

Fig. 3 Box plot for showing rainfall variability

the long-term mean (calculated over the 40-year period, i.e., 1970 to 2010) in some of the time in 11 stations. Furthermore, there appears to have been interventions in most of the stations (about eight) from 1982, resulting in a generally downward trend. The most probable dates (months since January 1970) for the observed interventions were determined and the step change analysis was carried to validate the observed intervention. The intervention dates and the corresponding step change analysis results are given in Table 4. It appears that the test statistic (Z values) are less than the critical value of 1.96 (5 %) in all 12 stations, suggesting that the CUSUM values cannot be confirmed. These results imply that the rainfall time series in Kariba catchment area come from the same climatological region and the area experiences an oscillatory hydrometeorological signal that has no apparent shifts over the 40-year period.

4.2.2 Homogeneity tests

Annual total rainfall amounts at each of the 13 stations was tested for homogeneity by the four absolute test methods reported in, e.g., Wijngaard et al. (2003), i.e., SNHT, BRT, PT, and VNT, and the results are given in Table 5. As reported in, e.g., Wijngaard et al. (2003), Feng et al. (2004), and Sahin and Cigizoglu (2010), the absolute tests considered here could have different sensitivities to changes in rainfall series. As a result, there are apparent differences in test results across the stations as illustrated in Table 5. The VNT scored four inhomogeneities; SNHT scored two inhomogeneities while PT and BRT scored one inhomogeneities each. Additionally, based on the Wijngaard et al. (2003) classification, the present study distinguished the inhomogeneities across the 13 stations by categorizing them

Table 3 Normality tests for annual, seasonal rainfall totals

Type of test and parameter of interest		Karoi	Hwange	Gokwe	Binga	Tsholotsho	Lupane	Nkayi	Mhondoro	Chibhero	Kariba	Victoria Falls	Kwekwe	Kadoma
Shapiro-Wilk	Annual	0.009	0.002	0.533	0.741	0.009	0.375	0.089	0.227	0.072	0.307	0.000	0.249	0.367
	DJF	0.210	0.322	0.483	0.447	0.026	0.231	0.439	0.008	0.174	0.922	0.045	0.134	0.647
Anderson-Darling	Annual	0.024	0.105	0.797	0.845	0.061	0.443	0.134	0.165	0.043	0.404	0.008	0.461	0.507
	DJF	0.282	0.478	0.574	0.214	0.055	0.308	0.683	0.206	0.214	0.974	0.017	0.038	0.476
Lilliefors	Annual	0.074	0.358	0.936	0.700	0.017	0.518	0.139	0.391	0.100	0.508	0.096	0.462	0.275
	DJF	0.223	0.375	0.652	0.205	0.218	0.351	0.683	0.325	0.069	0.996	0.000	0.040	0.503
Jarque-Bera	Annual	0.153	0.000	0.630	0.648	0.000	0.551	0.080	0.843	0.287	0.560	0.000	0.377	0.455
	DJF	0.370	0.525	0.433	0.705	0.313	0.603	0.551	0.000	0.432	0.814	0.392	0.640	0.784
Number of passes		5	6	8	8	4	8	8	6	6	8	2	6	8

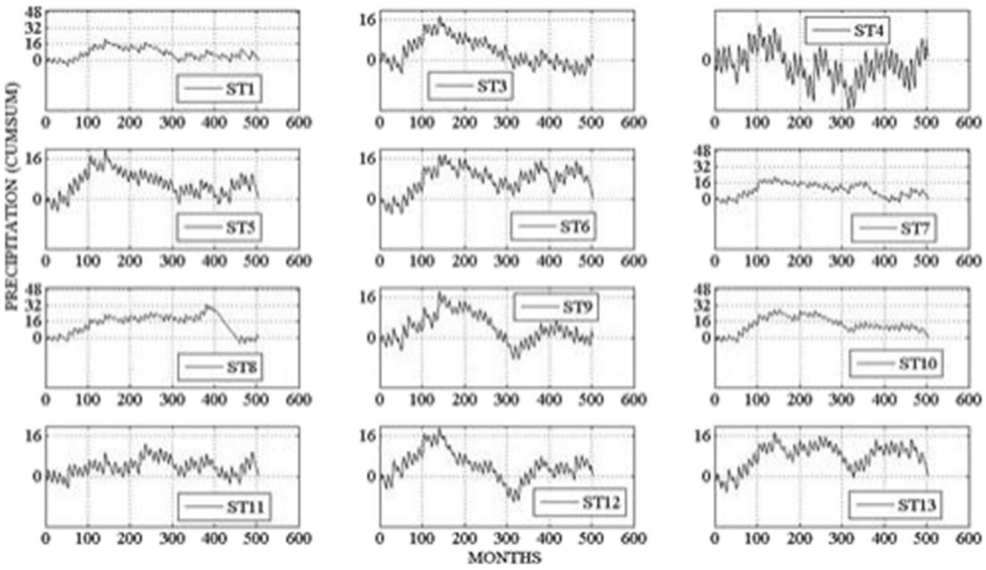

Fig. 4 CUSUM plot for rainfall in 12 stations

depending on the number of absolute tests rejecting the null hypothesis at the 5 % significance level, i.e., (a) class A, zero or one rejection; (b) class B, two rejections; and (c) class C, three or more rejections.

As shown in Table 5, Mhondoro and Tsholotsho stations are suspect (class C) and doubtful (class B), respectively, and all the other stations are useful (class A). This means that most of the stations considered in the present study seem to be homogeneous (and that the inherent heterogeneity amplitude that could be present is subtle) and therefore credible for trends and variability analysis. The heterogeneity present in Mhondoro suggest that any trends present in the Mhondoro rainfall data ought to be considered with caution or disregarded unless the magnitude of the trend is sufficiently large and this has to be supported with a priori information regarding the presence of climatic signal rather than artificial excursions.

Given in Table 6 are the results of the SNHT, BRT, PT, and VNT tests applied to DJF rainfall totals. The BRT and VNT characterize DJF rainfall at Hwange, Gokwe, and Chibhero stations to be inhomogeneous. These stations are in close proximity to Mhondoro station. Similarly, the DJF rainfall at the 13 stations has been characterized into two nominal classes A and B. Furthermore, Hwange, Gokwe, and Chibhero stations belong to class B category while the rest of the stations are class A category. These results suggest that trend and variability analysis of the DJF rainfall totals could be considered plausible. As a result, trend analysis of summer (DFJ) rainfall totals described in the present study inherently characterizes the nature of rainfall across the Lake Kariba catchment region of the Zambezi river basin.

Table 4 Step change analysis using the rank-sum method

Stations	Parameter			
	Break point (month)	*P* value	*h* value	*Z* value
Karoi	144	0.15	0	1.45
Gokwe	144	0.16	0	1.40
Binga	112	0.22	0	1.24
Tsholotsho	144	0.22	0	1.23
Lupane	144	0.16	0	1.40
Nkayi	128	0.14	0	1.48
Mhondoro	384	0.09	0	−1.68
Chibhero	144	0.32	0	0.99
Kariba	144	0.18	0	1.35
Victoria Falls	240	0.19	0	1.30
Kwekwe	144	0.30	0	1.03
Kadoma Cotton	144	0.13	0	1.51

4.3 Trend analysis

4.3.1 Annual trends

Results of the MK test for annual trends of precipitation in the Kariba catchment area, Zambezi basin, for the period 1970 to 2010 are shown in Table 7. All the stations with the exception of Mhondoro exhibit insignificant trends, suggesting that the probability distribution of the geophysical process driving the variability of rainfall totals has not changed over time. Our results corroborate those reported in Kampata et al. (2008) who used non-intervened series of rainfall in the hindstream of the upper Zambezi River Basin in Zambia. This underlying similarity arises due to the fact that the study region reported in Kampata et al. (2008) belongs to the same climate regime as the current study region. Using the KM test, it can be noticed that both positive (~62 %) and negative (~38 %) trends were

Table 5 Absolute homogeneity test for annual averaged rainfall totals

Type of test and parameter of interest		Karoi	Hwange	Gokwe	Binga	Tsholotsho	Lupane	Nkayi	Mhondoro	Chibhero	Kariba	Victoria Falls	Kwekwe	Kadoma Cotton
Pettit	K	102	159.0	102.0	120.0	168.0	100.0	144.0	214.0	136.0	184.0	84.0	130.0	102.0
	P	0.63	0.13	0.63	0.44	0.11	0.65	0.24	0.02	0.30	0.07	0.83	0.35	0.62
SNHT	T_0	7.68	5.17	3.53	2.64	12.91	3.16	4.69	13.28	5.16	7.23	19.47	4.71	3.35
	P	0.10	0.25	0.49	0.74	0.04	0.61	0.30	0.001	0.22	0.08	0.001	0.28	0.55
Buishand	Q	5.29	6.51	5.21	4.66	7.25	4.21	6.77	9.78	6.70	7.93	5.85	5.83	4.19
	P	0.40	0.16	0.41	0.55	0.09	0.67	0.14	0.01	0.15	0.06	0.27	0.28	0.67
von Neumann	N	1.92	1.88	1.83	2.04	1.38	1.87	1.72	1.04	1.59	1.24	1.67	1.37	1.66
	P	0.39	0.34	0.29	0.55	0.02	0.34	0.18	0.00	0.09	0.01	0.13	0.02	0.14
Test class		A	A	A	A	B	A	A	C	A	A	A	A	A

Table 6 Homogeneity tests for seasonal data

Type of test and parameter of interest		Karoi	Hwange	Gokwe	Binga	Tsholotsho	Lupane	Nkayi	Mhondoro	Chibhero	Kariba	Victoria Falls	Kwekwe	Kadoma Cotton
Pettit	K	74.0	168.0	124.0	74.0	90.0	76.0	104.0	90.0	146.0	170.0	86.0	140.0	96.0
	P	0.94	0.14	0.45	0.93	0.81	0.92	0.65	0.81	0.26	0.13	0.84	0.32	0.74
SNHT	T_0	2.37	8.64	8.92	7.50	2.15	7.49	2.34	3.02	10.93	6.04	3.59	5.83	4.25
	P	0.78	0.03	0.04	0.10	0.84	0.10	0.82	0.59	0.01	0.15	0.55	0.17	0.37
Buishand	Q	4.57	8.21	5.39	3.74	4.11	3.69	4.53	5.15	5.41	6.79	3.42	5.26	4.25
	P	0.58	0.05	0.38	0.79	0.71	0.82	0.59	0.44	0.38	0.16	0.87	0.41	0.67
Von Neumann	N	2.38	1.41	1.44	2.22	2.71	2.04	1.96	2.36	1.43	6.90	2.14	2.10	1.87
	P	0.90	0.02	0.03	0.76	0.71	0.55	0.44	0.89	0.03	0.50	0.68	0.62	0.34
Test class		A	B	B	A	A	A	A	A	B	A	A	A	A

Table 7 Annual rainfall trend test statistics for significant trends at α=0.05

Station name	Mann-Kendall test			Sen's slope		*h* values
	KENDALL τ	*P* values (two-tailed)	*Z* values	*P* values (two-tailed)	*b*	
Karoi	0.04	0.73	0.35	0.25	0.005	0
Hwange	0.05	0.65	0.45	0.89	0.005	0
Gokwe	−0.02	0.87	−0.17	0.40	−0.002	0
Binga	0.09	0.43	0.80	0.87	0.012	0
Tsholotsho	0.10	0.38	0.89	0.54	0.013	0
Lupane	0.00	1.00	0.00	0.45	0.000	0
Nkayi	0.08	0.49	0.69	0.75	0.009	0
Mhondoro	−0.25	0.02	−2.30	0.11	−0.027	1
Chibhero	−0.05	0.68	−0.42	0.45	−0.007	0
Kariba	−0.03	0.80	−0.26	0.19	−0.008	0
Victoria Falls	0.05	0.63	0.48	0.29	0.006	0
Kwekwe	−0.01	0.94	−0.08	0.67	−0.004	0
Kadoma Cotton	0.02	0.88	0.15	0.43	0.003	0

identified in annual precipitation data (this is illustrated in Fig. 5). Based on the Theil-Sen's estimator, the magnitudes of the significant trends were determined to be in the range of about (−) 0.027 mm/year at Mhondoro station to (+) 0.013 mm per year at Tsholotsho station.

4.3.2 Seasonal trends

The seasonal trends in rainfall time series were assessed by applying the MK test to the DJF rainfall time series spanning 1970 to 2010. As depicted in Table 8, all the stations did not have any significant trend at the 95 % significance level. As shown in Table 8 and Fig. 5, there exist both negative (~69 %) and positive (31 %) insignificant trends, and this structure is a complete inverse compared to the annual distribution pattern. This means that the Kariba catchment area is becoming subtly drier. This scenario might impact negatively on, e.g., the agricultural and livestock production activities (especially those activities that are time critical) in the area. In addition, decisions related to water management will be impacted due to the associated reduction of water

Table 8 Summer (DJF) rainfall trend test statistics for significant trends at $\boldsymbol{\alpha}$=0.05

Station name	Mann-Kendall test			Sen's slope		*h* values
	Kendall τ	*P* values (two-tailed)	*Z* values	*P* values (two-tailed)	*b*	
Karoi	0.04	0.75	0.33	0.87	0.005	0
Hwange	−0.18	0.28	−1.08	0.63	−0.016	0
Gokwe	−0.06	0.62	−0.51	0.46	−0.007	0
Binga	−0.06	0.59	−0.54	0.40	−0.010	0
Tsholotsho	0.01	0.91	0.11	0.91	0.001	0
Lupane	−0.03	0.76	−0.30	0.91	−0.004	0
Nkayi	0.10	0.35	0.93	0.40	0.013	0
Mhondoro	−0.01	0.93	−0.09	0.66	−0.001	0
Chibhero	0.08	0.44	0.77	0.91	0.011	0
Kariba	−0.17	0.12	−1.57	0.25	−0.022	0
Victoria Falls	−0.03	0.76	−0.30	0.16	−0.003	0
Kwekwe	−0.07	0.50	−0.67	0.20	−0.012	0
Kadoma Cotton	−0.02	0.87	−0.16	0.43	−0.001	0

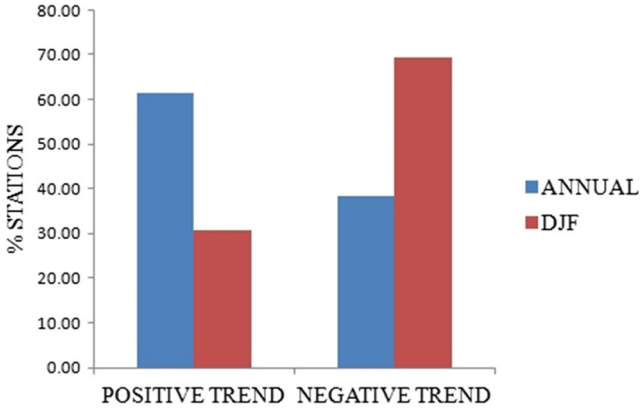

Fig. 5 Distribution of positive and negative trends at the 95 % confidence level using the Mann-Kendall test for the annual and seasonal rainfall mean totals (1970–2010)

levels in Lake Kariba. This subtle declining DJF rainfall, high variability, and the low statistical significance would often lead to underestimating the importance of climate signals (trends) that could be very catastrophic to society and the economy. The magnitude of the seasonal trends inherent in the DJF series in the Kariba catchment area ranges between −0.022 mm to + 0.013 mm per annum at Kariba and Nkayi stations, respectively.

4.4 Coherence of rainfall variability across stations

The CWT and WC derived from the Morlet continuous wavelet transform have been used to examine the nature of monthly total rainfall variability patterns across the

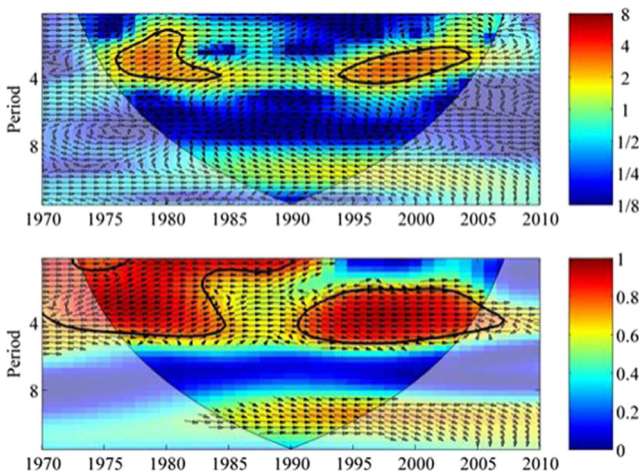

Fig. 6 Cross wavelet transform (*top*) and squared wavelet coherence (*below*) for rainfall between Karoi and Chibhero stations. Time (in years) is plotted on the horizontal axis while the period (in years) is plotted on the vertical axis. Color codes from *dark blue* (low values) to *dark red* (high values). The thick black contour designates the 5 % significance level against red noise and the lighter curve is the cone of influence (COI) that delimits the region not influenced by edge effects

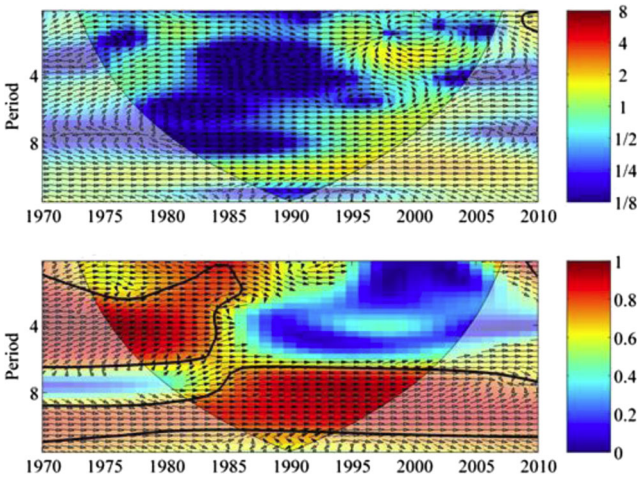

Fig. 7 Same as Fig. 6 but for rainfall between Tsholotsho and Nkayi

Kariba catchment area by assessing the presence of common power and the relative phase in the time-frequency space. In particular, the phase relationships between standardized rainfall records are explored given that they have common climatology. The Monte Carlo method [using 1000 ensemble surrogate data set pairs of the red noise based on the lag-one autoregressive (AR1) model coefficients of the standardized rainfall data sets] was used to compute the statistical significance (5 %) of CWT and WC. In the wavelet space, the rainfall variability in the northern region of the Kariba catchment area is depicted in Fig. 6. As illustrated in Fig. 6, the CWT of the standardized rainfall records at Karoi and Chibhero stations have constant in-phase and high common power (at 5 % significance level) during 1978–1983 and 1995–2003. There is, however, a larger area with phase-lock deviation outside the 5 % significance level. This implies that there are unreliable phase lags in rainfall between the two northern stations.

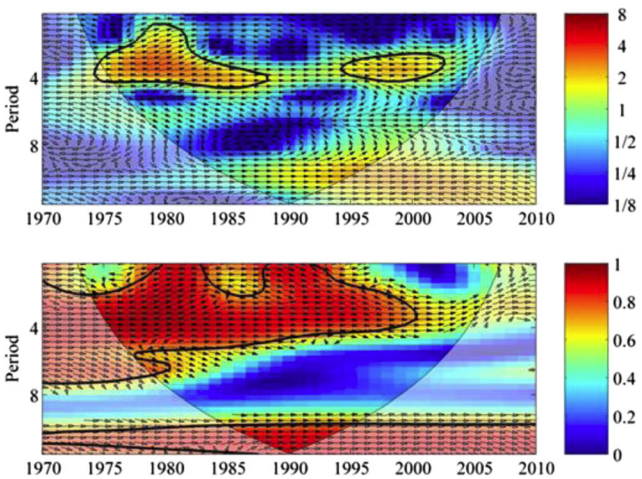

Fig. 8 Same as Fig. 6 but for rainfall between Mhondoro and Chibhero stations

Furthermore, the WC depicts larger sections with 5 % significance level exhibiting in-phase relationship, suggesting causality in the rainfall fluctuations. Overall, the modes of rainfall variability in the northern region of the Kariba catchment area are wavelengths varying from about 2 to 4 years.

As depicted in Fig. 7, rainfall fluctuations in the southern part of the Kariba catchment area (Tsholotsho and Nkayi stations) do not show high common power (at 5 % significance level) based on the CWT coefficients (top panel). However, the rainfall variability exhibit insignificant locked in-phase oscillatory modes at two wavelength bands varying from 2 to 6 years and 8–11 years around 1975 to 1985 and 1985 to 2002, respectively. The eastern part (Mhondoro and Chibhero stations) of the Kariba catchment area exhibits significant high power and constant in-phase around 1975–1985 and 1995–2002 (see Fig. 8). As shown in the bottom panel of Fig. 8, there is a larger section of the wavelet space with significant coherent oscillatory modes at varying wavelengths of 2–6 and 10–12 years between 1975 and 1998. This suggests that the rainfall variability as recorded in Mhondoro mirror the rainfall records at Chibhero station.

Rainfall variability for stations in the western part of the Kariba catchment area, i.e., Victoria Falls and Binga stations, are depicted in Fig. 9. The top panel illustrates that rainfall fluctuations at Victoria Falls and Binga stations have small sections in the wavelet space with significant common high power at timescales of 4 and 10 years. Sections with 5 % significance level are locked in-phase. The coherency in oscillatory modes (see bottom panel of Fig. 9) occurs at wavelengths above 8 years while the locked in-phase oscillatory modes appear between 1982 and 1995.

Figure 10 depicts the CWT (top panel) and WC (bottom panel) for rainfall records in the central part (Gokwe and Kariba) of the Kariba catchment area. As illustrated in the CWT, areas of significant high common power occur at

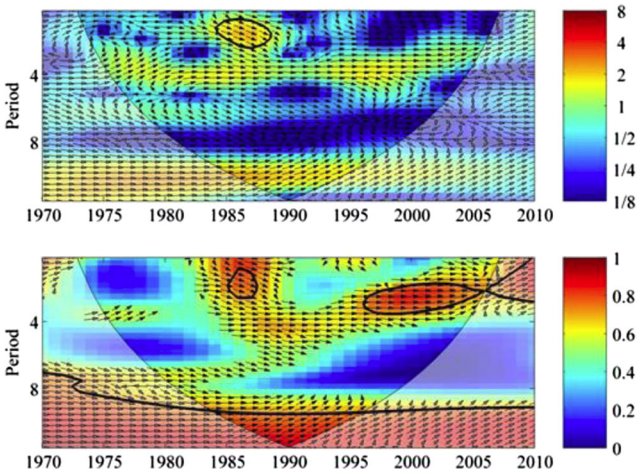

Fig. 10 Same as Fig. 6 but for rainfall at Gokwe and Kariba stations

wavelength region of approximately 2–3 years centered around 1985. Furthermore, there are weak in-phase oscillatory modes of rainfall records at Gokwe and Kariba stations. Gokwe and Kariba stations have the shortest baseline implying that the fluctuations in the rainfall series ought to mirror each other. On the other hand, the WC of the rainfall time series at Gokwe and Kariba stations exhibit high coherence around 1985 (at a wavelength of 2–3 years) and between 1995 and 2005 (wavelength centered at 4 years). Compared to the short baseline (i.e., between Gokwe and Kariba stations), Karoi and Tsholotsho stations have a relatively long north–south baseline. The relationship between rainfall records at Karoi and Tsholotsho stations is depicted in Fig. 11. The CWT (top panel in Fig. 11) illustrates that the significant locked in-phase rainfall oscillatory modes and common power with time scale of 4 years occurred around 1998. Compared to CWT, the WC (bottom panel in Fig. 11) depicts a larger section of significant coherency with marked locked in-phase rainfall fluctuations, suggesting that rainfall variability at the various stations across the Kariba catchment area exhibits

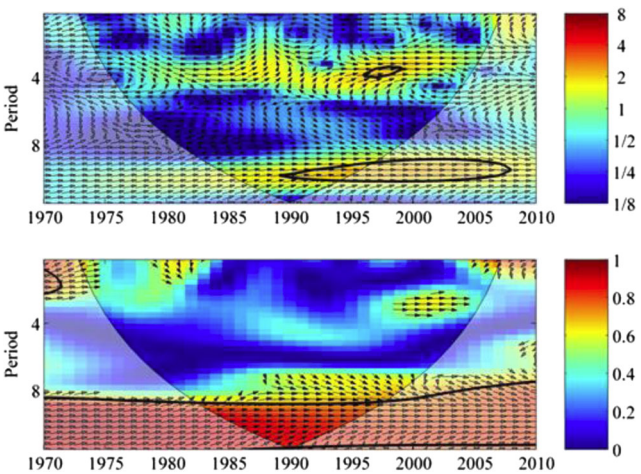

Fig. 9 Same as Fig. 6 but for rainfall at Victoria Falls and Binga stations

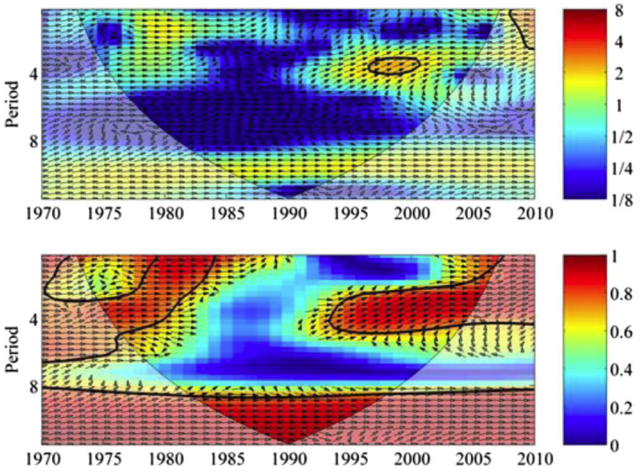

Fig. 11 Same as Fig. 6 but for rainfall between Karoi and Tsholotsho (long north–south baseline) stations

Table 9 Characteristic of rainfall variability based on wavelet-based parameters across the Kariba catchment region

Region	Significant common power	Significant constant phase	Wavelength (years)	Time span
North	Present	In-phase	2–4	1975–1983; 1995–2003
South	Absent	In-phase	2–6; 8–11	1975–1985; 1985–2002
East	Present	In-phase	2–6; 10–12	1975–1985; 1995–2002
West	Present	In-phase	4–10	1982–1995
Central	Present	In-phase	2–3	1985; 1995–2005

spatially independent and temporally independent constant phases. Overall, the characteristics of rainfall variability in the Kariba catchment area based on the wavelet-based parameters are summarized as in Table 9.

5 Conclusions

The significance of analyzing the variability of rainfall for weather and climate studies has been underscored by various researchers from the diverse scientific community. In the present study, rainfall data from a network of 13 stations across the Kariba catchment area in the Zambezi river basin has been analyzed. Based on the four decades of rainfall data, the following conclusions can be drawn:

(a) All network stations in the Kariba catchment exhibited similar annual and seasonal (DJF) rainfall variability pattern.
(b) Annual and seasonal rainfall series across the network of stations over Lake Kariba catchment area (about 78 %) demonstrated normal distribution.
(c) There were no apparent significant shifts in the annual and seasonal rainfall data in the Kariba catchment area based on the CUSUM and rank-sum test analysis.
(d) Annual and seasonal rainfall data from most of the stations were homogeneous. Based on the Wijngaard et al. (2003) classification, the network of station considered in the present study were category A (useful) and B (doubtful) stations implying that trend and variability analysis results using the station time series would be considered plausible.
(e) The annual and seasonal rainfall series in the Kariba catchment area have non-significant positive and negative trends.
(f) Most network stations considered in the present study exhibit coherent oscillatory modes that are constantly locked in-phase in the Morlet wavelet space.

The current study is a step towards bridging the gap in rainfall variability characterization in the Kariba catchment area. In particular, these results would be valuable since local-scale rainfall variability can lead to sudden changes in water availability in the surface and sub-surface hydrologic systems thereby significantly affecting agriculture, livestock, water supply, and hydropower sectors—the social economic livelihoods over the study area. Future studies focusing on investigating the (a) occurrence of extreme events and (b) link between rainfall variability and tele-connection patterns such as the Intertropical Convergence Zone (ITCZ), El Niño and La Niña (ENSO), and Indian Ocean Dipole (IOD) are recommended.

References

Alexandersson H (1986) A homogeneity test applied to precipitation data. J Climatol 6:661–675

Alexandersson H, Moberg A (1997) Homogenization of SWEDISH temperature data. Part I: homogeneity test for linear trends. Int J Climatol 17(1):25–34

Beilfuss RD (2012) A risky climate for Southern Africa hydro. Hydrological risks and consequences for Zambezi River Basin Dams. International Rivers, Beckeley

Buishand TA (1982) Some methods for testing the homogeneity of rainfall records. J Hydrol 58:11–27

Cannarozzo M, Noto LV, Viola F (2006) Spatial distribution of rainfall trends in Sicily (1921–2000). Phys Chem Earth A/B/C 31(18): 1201–1211

Cook KH (2000) The South Indian convergence zone and interannual rainfall variability over Southern Africa. J Clim 13(1):3789–3804

Cook C, Reason CJC, Hewitson BC (2004) Wet and dry spells within particularly wet and dry summers in the South African summer rainfall region. Clim Res 26:17–31

Costa AC, Soares A (2009) Homogenization of climate data: review and new perspectives using geostatistics. Math Geosci 41(3):291–305

De Luis M, Raventos J, Gonzalez-Hidalgo JC, Sanchez JR, Cortina J (2000) Spatial analysis of rainfall trends in Valencia (east of Spain). Int J Climatol 20(12):1451–1469

Feng S, Hu Q, Qian W (2004) Quality control of daily meteorological data in China, 1951–2000: a new dataset. Int J Climatol 4:853–870

Grinsted A, Moore JC, Jevrejeva S (2004) Application of the cross wavelet transform and wavelet coherence to geophysical time series. Nonlinear Process Geophys 11:561–566

Helsel DR, Hirsch RM (2002) Statistical methods in water resources. United States Geological Survey 524

IPCC (2007) In: Parry ML, Canziani OF, Palutokof JP, van der Linden PJ, Hanson CE (eds) Climate Change 2007: impacts, adaptation and vulnerability. Contributions of Working Group II to the fourth

assessment of the Intergovernmental Panel on Climate Change. Cambridge University Press, Cambridge

Kampata JM, Parida BP, Moalafhi DB (2008) Trend analysis of rainfall in the headstreams of the Zambezi River Basin in Zambia. Phys Chem Earth 33:621–625

Kendall M (1975) Rank correlation methods. Charles Griffin, London

Lindesay JA (1988) South African rainfall, the Southern Oscillation and a Southern Hemisphere semi-annual cycle. J Climatol 8:17–30

Liu Y, Wang K, Yu C, He Y, Zhou Y, Liang M, Wang L, Jiang T (2008) Regional homogeneity, functional connectivity and imaging markers of Alzheimer's disease: a review of resting-state fMRI studies. Neuropsychologia 46(6):1648–1656

Mann HB (1945) Nonparametric tests against trend. Econometrica 13(3): 245–259

Maraun D, Kurths J (2004) Cross wavelet analysis: significance testing and pitfalls. Nonlinear Process Geophys 11:505–514

Maraun D, Kurths J, Holschneider M (2007) Nonstationary Gaussian processes in wavelet domain: synthesis, estimation, and significance testing. Phys Rev E 75

Mason SJ, Joubert AM (1997) Simulated changes in extreme rainfall over southern Africa. Int J Climatol 17:291–301

Mason SJ, Jury MR (1997) Climate variability and change over southern Africa: a reflection on underlying processes. Prog Phys Geogr 21: 23–50

Mazvidza DZ, Sakala W, Makupe H (2000) Water transfer schemes due to uneven spatial distribution: development projects. In Tumbare MJ (ed) Management of river basins and dams: the Zambezi River Basin. AA Balkema: Rotterdam/Brook fields

Mazvimavi D, Wolski P (2006) Long-term variations of annual flows of the Okavango and Zambezi Rivers. Phys Chem Earth 31:951–994

Modarres R, da Silva RVP (2007) Rainfall trends in arid and semi-arid regions of Iran. J Arid Environ 70(2):344–355

Ngongondo CS (2006) An analysis of long-term rainfall variability, trends and ground water availability in the Mulunguzi river catchment area, Zomba mountain, southern Malawi. Quat Int 148:45–50

Nicholson SE, Entekhabi D (1987) Rainfall variability in equatorial and southern Africa: relationships with sea-surface temperatures along southwestern coast of Africa. J Clim Appl Meteorol 26:561–578

Nsubuga FWN, Olwoch JM, Rautenbach CJ (2011) Climatic trends at Namulonge in Uganda: 1947–2009. J Geography Geol 3:119–131

Parida BP, Moalafhi DB, Kenabatho PK (2003) Effect of urbanization on runoff coefficient: a case of Notwane catchment in Botswana. In: Proceedings of the International Conference on Water and Environment (WE-2003), Bhopal, "Watershed Hydrology". Allied Publishers Pvt Ltd: 123–131

Partal T, Kahya E (2006) Trend analysis in Turkish precipitation data. Hydrol Process 20:2011–2026

Peterson TC, Easterling DR, Karl TR, Groisman P, Nicholls N, Plummer N, Torok S, Auer I, Boehm R, Gullett D, Vincent L, Heinof R, Tuomenvirta H, Mestre O, Szentimreyh S, Salinger J, Førland EJ, Hanssen-Bauer H, Alexandersson H, Jones P, Parker D (1998) Homogeneity adjustments of *in situ* atmospheric climate data: a review. Int J Climatol 18(13):1493–1517

Pettit AN (1979) A non-parametric approach to the change-point detection. Appl Stat 28:126–135

Quesenberry CP (1986) Some transformation methods in goodness-of-fit. In: D'Agostino RB, Stephens MA (eds) Goodness-of-fit techniques. Marcel D, New York, pp 235–277

Reason CJC, Rouault M (2002) ENSO-like decadal patterns and South African rainfall. Geophys Res Lett 29(13):16–1 – 16–4

Reason CJC, Allan RJ, Lindesay JA, Ansell TJ (2000) ENSO and climatic signals across the Indian Ocean basin in the global context: part 1, interannual composite patterns. Int J Climatol 20:1285–1327

Sahin S, Cigizoglu HK (2010) Homogeneity analysis of Turkish meteorological data set. Hydrol Sci Hydrol Process 24(8):981–992

Sen PK (1968) Estimates of the regression coefficient based on Kendall's Tau. J Am Stat Assoc 1379–1389

Shannon LV, Lutjeharms JRE, Nelson G (1990) Causative mechanisms for intra-annual and interannual variability in the marine environment around southern Africa. South Afr J Sci 86:356–373

Sharma TC, Nyumbu IL (1985) Some hydrologic characteristics of the Upper Zambezi Basin. In: Handlos WL, Howard GW (eds). Development prospects for the Zambezi Valley in Zambia. Lusaka. Kafue Basin Research Committee of the University of Zambia 29–43

Solomon S, Qin D, Manning M, Alley RB, Berntsen T, Blindoff NL, Chen Z, Chidthaisong A, Gregory JM, Hegerl GC, Heimann M, Hewitson B, Hoskins BJ, Joos F, Jouzel J, Kattsov V, Lohmann U, Matsuno T, Molina M, Solomon S, Qin D, Manning M, Chen Z, Marquis M, Averyt KB, Tignor M, Miller HL et al (2007) Technical summary. In: Climate Change 2007: The Physical Science Basis. In: Contribution of Working Group 1 to the Fourth Assessment Report of the Intergovernmental Panel on Climate Change. Cambridge University Press, Cambridge

Theil H (1950) A rank-invariant method of linear and polynomial regression analysis, I, II, III. Ned Akad Wetensch Proc 53:386–392, 521–525 and 1397–1412

Torrence C, Compo GP (1998) A practical guide to wavelet analysis. Bull Am Meteorol Soc 79:61–78

Tysen PD (1986) Climatic change and variability in Southern Africa. Oxford University Press, Cape Town

Von Neumann J (1941) Distribution of the ratio of the mean square successive difference to the variance. Ann Math Stat 13:367–395

Wijngaard JB, Klein Tank AMG, Konnen GP (2003) Homogeneity of 20th century European daily temperature and precipitation series. Int J Climatol 23(6):679–692

Yue S, Hashimo M (2003) Long term trends of annual and monthly precipitation in Japan. JAWRA J Am Water Resourc Assoc 3(3): 587–596